Simulation of shot noise effects in the EIC strong hadron cooling accelerator using real number of electrons

Ji Qiang[1] **and Erdong Wang**[2]

[1]Lawrence Berkeley National Laboratory, Berkeley, CA, USA
[2]Brookhaven National Laboratory, Upton, NY, USA

E-mail: jqiang@lbl.gov

Abstract. In the electron ion collider design, in order to achieve the peak luminosity $10^{34}/cm^2/s$ with a reasonable lifetime, an efficient coherent electron cooling scheme was proposed to reduce the hadron beam emittance growth. Such a cooling scheme requires a good electron beam quality with a small energy spread. However, the shot noise in the electron beam through the accelerator might be amplified due to the microbunching instability and degrades the electron beam quality in the modulator section of the strong hadron cooling channel and correspondingly cooling rate. In this study, we report on self-consistent simulations of these effects using a real number of electrons to capture the details of shot noise and analysis of the shot noise growth through the accelerator.

1. Introduction

The Electron-Ion-Collider (EIC) as the next generation nuclear physics collider demands high luminosity ($10^{34}/cm^2/s$) during the collision. For such a high luminosity, the intrabeam scattering effects inside the hadron beam and other collective effects can cause beam emittance growth and lifetime degradation. In order to maintain the high luminosity for sufficiently long collision time, the hadron beam has to be cooled. At present, the coherent electron cooling is the most promising method to cool the hadron beam in the EIC project due to the high cooling rate [1]. An Energy Recovery Linac (ERL) has been actively studied to provide the intense electron beam needed for the coherent electron cooling [2]. The shot noise inside the electron beam could be amplified in this accelerator through the process of microbunching instability. The amplification of the initial electron beam shot noise has been observed and studied in other accelerators such as LCLS [3, 4]. The amplified shot noise in the short wavelength regime will smear the hadron modulation signal and degrade the cooling rate. In this paper, we studied the shot noise evolution through the cooling accelerator using the self-consistent high precision macroparticle tracking with the real number of electrons and analyzed the shot noise growth through the accelerator.

2. Computational tool

The computational tool used in this study is a massive parallel beam dynamics simulation framework, IMPACT, code suite. It includes two parallel particle-in-cell tracking codes:

IMPACT-T and IMPACT-Z [5, 6, 7]. The IMPACT-T code is a three-dimensional macroparticle tracking code using time as the independent variable. It simulates the electron beam emission from the photocathode and the electron beam transport and acceleration through injector and accelerator including the self-consistent space-charge effects. Here, the space charge effects were computed by solving the three-dimensional Poisson equation in the moving beam frame using an integrated Greens function method [8]. The fast Fourier transform (FFT) is used to compute the discrete convolution efficiently. The IMPACT-Z code is a parallel particle-in-cell code for modeling high intensity/high brightness beams in linear and circular accelerators using longitudinal position z as the independent variable. The computational model in the IMPACT-Z code includes exact transfer map through a drift, linear transfer map for the hard edge quadrupole with energy dependence, transfer map for dipole, linear transfer matrix through RF superconducting cavity, thin lens kick model for sextupole, self-consistent 3D space-charge effects, 1D steady state and transient coherent synchrotron radiation (CSR) effects, incoherent synchrotron radiation (ISR) effects through bending magnet, longitudinal structure and resistive wall wakefields, and uncorrelated energy increase from analytical intrabeam scattering (IBS) model. The IMPACT code has been successfully applied to the x-ray light source accelerator and benchmarked with both the other codes and experimental measurements. In this study, we have used real number of electrons in the high precision simulation to capture the initial shot-noise of the electron beam.

3. Simulation of shot noise through the cooling accelerator

A schematic plot of the nominal strong hadron cooling accelerator is shown in Fig. 1 [2]. It consists of an injector, a merger, and a linac section. The injector consists of a DC gun, a

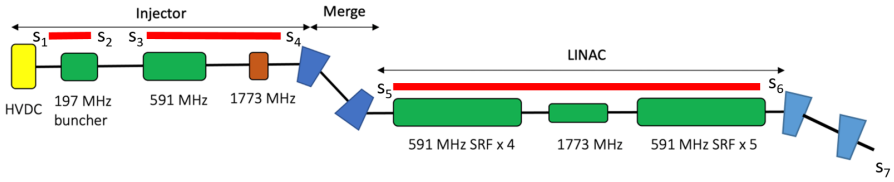

Figure 1. A layout of the nominal strong hadron cooling injector and linac.

197 MHz RF cavity buncher, a 591 MHz RF cavity booster, and a 1773 MHz 3rd harmonic linearizer. The merger consists of two 15 degree bending magnets. The linac consists of four 591 MHz accelerating cavities, another 1773 MHz harmonic linearizer, and another four 591 MHz cavities.

We carried out the high precision simulation using about 6.25 billion macroparticles for 1 nC charge and $64 \times 64 \times 2048$ grid points. Each macroparticle corresponds to a real electron. Using the real number of electrons in the simulation is to capture the details of shot noise inside the electron beam. In order to estimate the shot noise level of a group of macroparticles, we compute the relative current fluctuation level from the linear deposition of these macroparticles onto a one-dimensional grid. For a randomly sampled smooth distribution function, the relative RMS density fluctuation level on a grid point I can be obtained as:

$$\frac{\sigma(\bar{\rho}(x_I))}{\rho_I} = \sqrt{\frac{2}{3}}\frac{1}{\sqrt{N_{PI}}} \tag{1}$$

where N_{PI} is the number of macroparticles in grid cell I. This density fluctuation level represents the shot noise level of a group of macroparticles from the random sampling of a smooth function without any amplification. Figure 2 shows the final current profile and the relative current

fluctuation from the linear deposition of the macroparticles (real number of electrons) after transporting through the strong hadron cooling accelerator in the high precision simulation including both the space-charge effect and the CSR effect. Here, the relative current fluctuation is defined as $(I_s - I_{fit})/I_{fit}$. where I_s is the current from simulation and I_{fit} the current from fitting using a polynomial function. A relative current modulation with a wavelength of about 280 μm is seen from the relative current fluctuation. In order to view this modulation

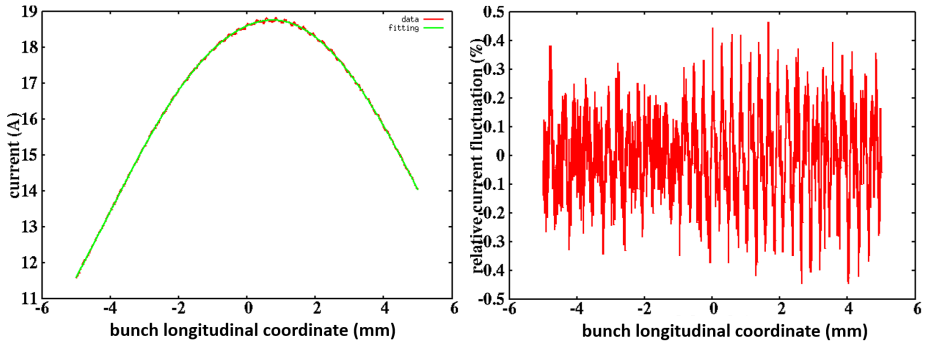

Figure 2. Final current profile (top) and relative current fluctuation (bottom) from the linear deposition of macroparticles at the end of the accelerator.

more clearly, Figure 3 shows the zoom-in current profile and relative current fluctuation for a small section of the electron beam. The relative RMS current fluctuation after removing the modulation is about 7.5×10^{-4}, which is at the same level as the relative current fluctuation from direct random sampling of the smooth fitting function. This suggests that the initial high frequency shot noise level has not been amplified through the nominal strong hadron cooling accelerator. Figure 4 shows the power spectral density of the relative current fluctuation (after

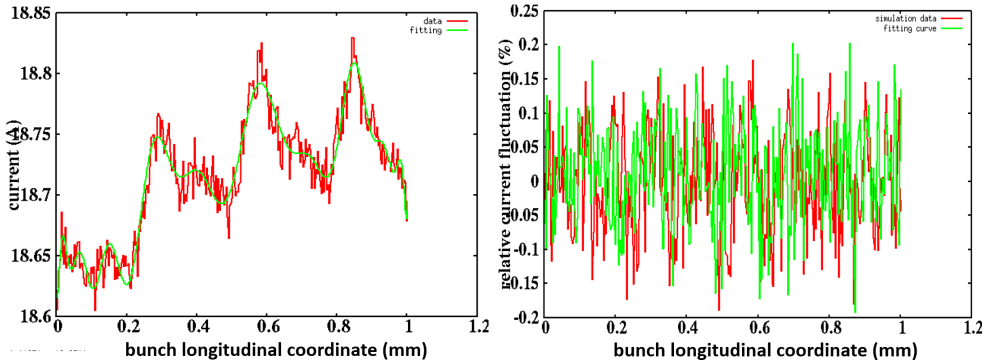

Figure 3. Zoom-in final current profile (top) and relative current fluctuation (bottom) from the simulation macroparticles and from the direct random sampling of the smooth fitting function.

removing the 280 μm modulation) of the electron beam through the nominal accelerator and of the direct random sampling of the smooth fitting function. The relative current fluctuations in both cases show the same level of power spectral density, which is consistent with the direct relative current fluctuations.

In the above high precision simulation, the longitudinal resolution is about 20 microns. This is larger than the longitudinal scale length interested in the strong hadron cooling (about a few microns). In order to further increase the longitudinal resolution, we selected a slice of 150 micron electron beam at 20 MeV, assuming a longitudinal periodic boundary condition with a

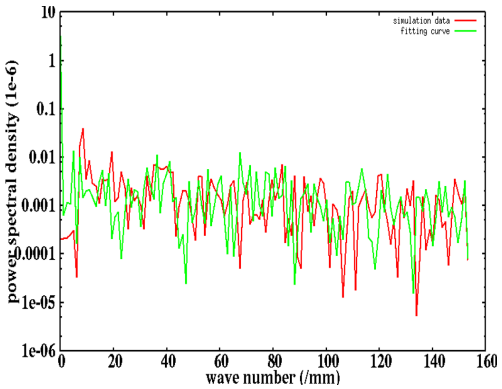

Figure 4. Power spectral density of the simulated relative current fluctuation and the random sampled relative current fluctuation.

transverse open boundary condition, and reran the simulation through the linac using the real number of electrons inside that slice of the beam and $64 \times 64 \times 513$ numerical grid points. The resultant 0.3 μm longitudinal resolution is sufficient for the few micron cooling interested scale length. Figure 5 shows the final current profile and the relative current fluctuation from that simulation macroparticles and from the random sampling of the smooth fitting function. The relative current fluctuation level at the end of the accelerator is the same as the fluctuation level from the direct random sampling. Figure 6 shows the power spectral density of the simulated

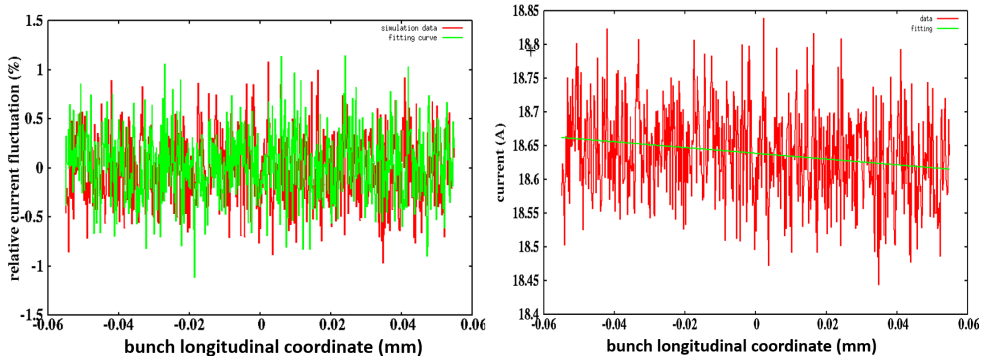

Figure 5. The final current profile (top) and relative current fluctuation (bottom) from the improved longitudinal resolution simulation macroparticles and from the direct sampling.

relative current fluctuation and the directly random sampled current fluctuation. The relative current fluctuation from the simulation macroparticles with improved longitudinal resolution shows the same level of power spectral density as the directly sampled fluctuation. This suggests that the high frequency shot noise down to the cooling length scale were not amplified through the linac.

4. Estimate of the microbunching instability gain

The shot noise inside the electron beam can be amplified through the accelerator due to the collective effects, especially, the space-charge effects. This is also called the microbunching instability. In the following, we use an analytical model based on the linearized Vlasov equation to estimate the gain of the microbunching instability.

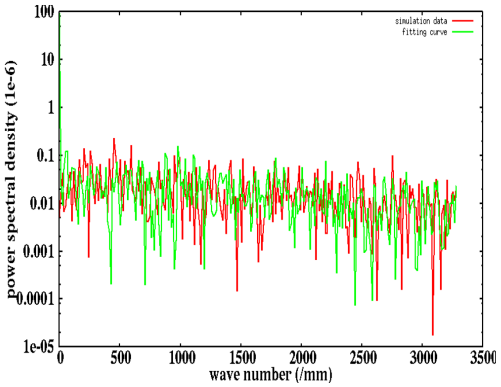

Figure 6. Power spectral density of the simulated current fluctuation and the random sampled fluctuation.

Assuming an electron beam with an initial current modulation factor b_0 at the entrance (s_1) to RF buncher cavity, the modulation factor at a location s of the accelerator can be obtained by solving the following integral equation [9, 10]:

$$b[k(s);s] \quad = \quad b_0[k(s);s] + \int_{s_1}^{s} K(\tau,s) b[k(\tau);\tau] d\tau \tag{2}$$

where the kernel of the above integral equation is given as:

$$\begin{aligned} K(\tau;s) \quad &= \quad ik(s)\hat{R}_{56}(\tau \rightarrow s)\frac{I(\tau)}{I_A}\frac{Z[k(\tau);\tau]}{\gamma_0} \times \\ &\exp\,(\,-\frac{k_0^2}{2}U^2\sigma_{\delta 0}^2) \end{aligned} \tag{3}$$

where $U(s,\tau) = C(s)R_{56}(s) - C(\tau)R_{56}(\tau)$, k the modulation wavenumber and the Alfvén current $I_A \simeq 17.045$ kA.

The above integral equation can be solved iteratively. Assuming that the electron beam is longitudinally frozen inside the injector and the linac sections and neglecting collective effects inside the mergers, we can calculate the final modulation factor at the exit of L3 (s_7) [11]. Figure 7 shows the microbunching instability gain at the end of the accelerator as a function

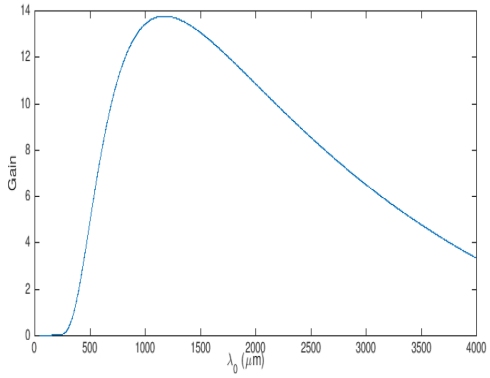

Figure 7. Microbunching instability gain as a function of initial modulation wavelength.

of the initial modulation wavelength. The microbunching gain attains maximum around 1000

micron initial modulation wavelength. Given the factor of 3 compression through the accelerator, this suggests that the final modulation wavelength should be around 300 microns. This is in consistent with the modulation wavelength observed in the above high precision simulation.

Acknowledgments
This work was supported by the U.S. Department of Energy under Contract No. DE-AC02-05CH11231 and used computer resources at the National Energy Research Scientific Computing Center.

References
[1] F. Willeke, "Electron-Ion Collider Conceptual Design Report 2021," doi:10.2172/1765663.
[2] E. Wang, et al., "Electron ion collider strong hadron coling injecor and ERL," in Proc. LINAC2022, Liverpool, UK, p. 7, 2022.
[3] D. Ratner, C. Behrens, Y. Ding, Z. Huang, A. Marinelli, T. Maxwell, and F. Zhou, Phys. Rev. ST Accel. Beams 18, 030704 (2015).
[4] J. Qiang, Y. Ding, P. Emma, Z. Huang, D. Ratner, T. O. Raubenheimer, F. Zhou, and M. Venturini, Phys. Rev. Accel. Beams 20, 054402 (2017).
[5] J. Qiang, R. D. Ryne, S. Habib, V. Decyk, J. Comput. Phys. **163**, 434, (2000).
[6] J. Qiang, S. Lidia, R. D. Ryne, and C. Limborg-Deprey, Phys. Rev. ST Accel. Beams **9**, 044204, (2006).
[7] J. Qiang, R. D. Ryne, M. Venturini, A. A. Zholents, and I. V. Pogorelov, Phys. Rev. ST Accel. Beams, vol. 12, 100702, (2009).
[8] J. Qiang, S. Lidia, R. D. Ryne, and C. Limborg-Deprey, Phys. Rev. ST Accel. Beams **10**, 129901, (2007).
[9] S. Heifets, G. Stupakov, and S. Krinsky, Phys. Rev. ST Accel. Beams, vol. 5, p. 064401, (2002).
[10] Z. Huang and K. J. Kim, Phys. Rev. ST Accel. Beams, vol. 5, 074401, (2002).
[11] B. Li and J. Qiang, Phys. Rev. Accel. Beams 23, 014403 (2020).